Statistical and preequilibrium γ-ray emission in heavy ion reactions at 25 MeV/nucleon

F. Amorini,[1,2] G. Cardella,[3,*] A. Di Pietro,[1] P. Figuera,[1] G. Lanzalone,[1,2] Lu Jun,[1] A. Musumarra,[1,4] M. Papa,[3] S. Pirrone,[3] F. Rizzo,[1,2] W. Tian,[1] and S. Tudisco[1,4]

[1]*INFN, Laboratorio Nazionale del Sud, Catania, Italy*

[2]*Dipartimento di Fisica e Astronomia, Università di Catania, Italy*

[3]*INFN, Sezione di Catania, Catania, Italy*

[4]*Dipartimento di Metodologie Fisiche e Chimiche per l'Ingegneria, Università di Catania, Catania, Italy*

(Received 24 June 2003; published 30 January 2004)

We measured γ-ray spectra in coincidence with charged particles for the reactions $^{40}Ca+^{48}Ca$, ^{46}Ti at beam energy of 25 MeV/nucleon. Events corresponding to reaction mechanisms from quasielastic to fusion were observed. In fusion and in inelastic reactions an enhancement in the γ-ray spectra is present in the energy region around 10 MeV for the ^{48}Ca target with respect to ^{46}Ti data. The analysis of the γ-ray spectra relative to ^{48}Ca and ^{46}Ti targets shows the persistence of the GDR up to an excitation energy around $4-5$ MeV/nucleon for the mass region around 60. This result was obtained by including, in the statistical calculations, corrections due to the open decay channels, the mass dependence of the GDR parameters, and isospin effects.

DOI: 10.1103/PhysRevC.69.014608 PACS number(s): 24.30.Cz, 24.60.Dr, 25.70.Jj

I. INTRODUCTION

The γ-ray energy spectra produced in heavy ion collisions carry detailed information on the excited systems populated in nuclear reactions. Low-energy γ-ray multiplicity [1], Giant Dipole Resonance (GDR) γ decay [2], and nucleon-nucleon bremsstrahlung [3], have been extensively studied in order to extract such information. Recently it has been suggested [4] to investigate through γ-ray spectra into the liquid-gas phase transition of nuclear matter. During this transition the nuclear matter cannot show a collective behavior and before the transition occurs, the collective excitations like the GDR should disappear. Therefore the detailed study of GDR at very high excitation energy can be useful to understand the behavior of nuclear matter close to the liquid-gas phase transition. Some measurements [5,6] show the GDR disappearance at an excitation energy (E^*_{cutoff}) of about $2-3$ MeV/nucleon, near the energy where the mixed liquid-gas phase is claimed to appear for mass around 200 [7]. We studied systems around mass 60 populated through the reactions $^{40}Ca+^{48}Ca$, ^{46}Ti at 25 MeV/nucleon beam energy [8], and we observed the presence of the GDR at excitation energies up to $4-5$ MeV/nucleon, about two times more than was previously measured. The difference in the limiting excitation energy measured in our work with respect to the previous ones agrees to the mass dependence of caloric curves recently analyzed by Natowitz *et al.* [9]. They noted in fact that the plateau of the caloric curve starts around 8 MeV/nucleon of excitation energy for mass between 30 and 60, whereas it is found around 4 MeV/nucleon for mass above 100 a.m.u.

In this work we will discuss in a more complete and detailed way the results concerning the study of the reactions $^{40}Ca+^{48}Ca$, ^{46}Ti at 25 MeV/nucleon [8]. The two systems with different N/Z ratio were studied to search for a possible dependence of the GDR limiting temperatures on the N/Z ratios [10]. Furthermore, the study of these two systems was also important to obtain complementary information on the preequilibrium γ-ray emission [11–18]. Such preequilibrium effects, which are produced by the fast charge equilibration in reactions between N/Z asymmetric projectile-target systems [16], can in fact affect the statistical analysis of the spectra. In our case the ^{46}Ti target ($N/Z=1.09$) has been used as a reference system to evidence the preequilibrium effects in the N/Z asymmetric $^{40}Ca(N/Z=1)+^{48}Ca(N/Z=1.4)$ reaction. We will discuss the evolution of such preequilibrium emission for the different reaction mechanisms observed. The results of preequilibrium analysis will be used to identify the energy region of the γ-ray spectra where the statistical analysis can be performed without problems. An error analysis will complete this paper showing the confidence level of our results. The paper is divided into four sections. In Sec. II, we describe the experimental setup and results. In Sec. III statistical calculations are presented together with data analysis. Section IV is devoted to the conclusive remarks.

II. EXPERIMENTAL APPARATUS AND RESULTS

The experiment was performed at the Superconducting Cyclotron of the Laboratori Nazionali del Sud (LNS) in Catania. A 25 MeV/nucleon beam of ^{40}Ca was used impinging on self-supporting 3 mg/cm^2 thick targets of ^{48}Ca, ^{46}Ti both 95% isotopically enriched. All the procedures concerning the targets from the storage phase to the mounting in the scattering chamber were realized under controlled atmosphere to avoid oxidation.

We used the multidetector system TRASMA [19]. In this apparatus γ rays are measured by using 63 BaF_2 detectors, arranged in nine clusters of seven crystals each. These clusters are positioned 25 cm far from the target at polar angles

*Electronic address: Cardella@ct.infn.it

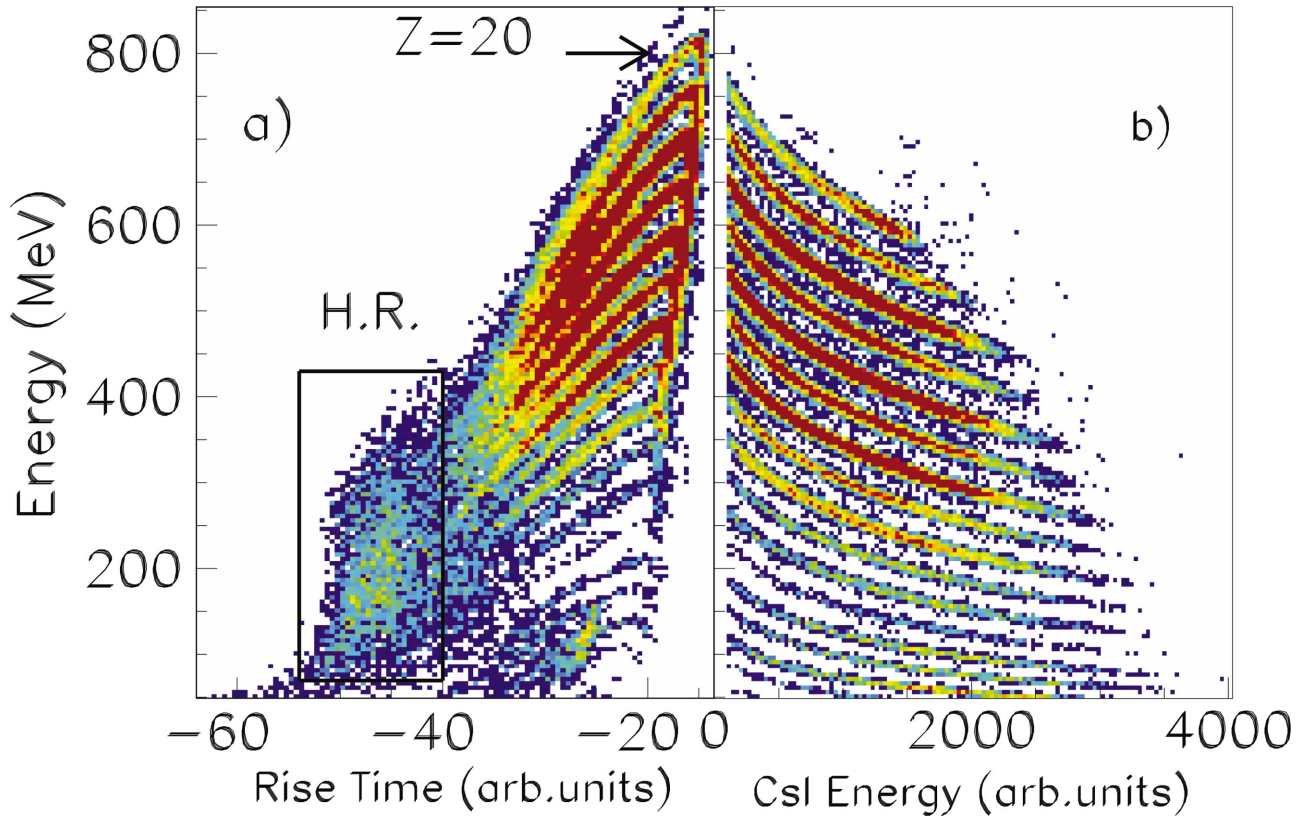

FIG. 1. (Color) (a) Energy "rise-time" scatter plot for the reaction ^{40}Ca+^{48}Ca at 25*A* MeV for particles stopped inside the silicon detector (300 μm thick) The box indicates the selected region of evaporation residues. (b) ΔE-E scatter plot for particles producing a signal in the CsI(Tl).

of 45°, 90°, and 135°, and with azimuthal angles of 0°, 90°, 180°, covering a total solid angle of about 3 sr. The experiments on the two targets were performed with the same experimental setup to allow a direct comparison of the data.

Detectors were calibrated during the experiment by using low-energy standard γ-ray sources (^{88}Y, ^{60}Co), and the 4.44 MeV γ rays obtained by the ^{241}Am-^{9}Be source. The reliability of our energy calibration method around the GDR energy has been checked in previous papers [20] by comparing GEANT simulations with cosmic rays and the 1.51 MeV γ ray from p+^{12}C reaction. Neutron subtraction was done using both time of flight and pulse shape information from BaF_2 detectors. The detector gain was checked by repeating the calibration procedure several times during the experiment and also by comparing (offline) the exponential slopes of the spectra for the different runs. The comparison between the calibration runs shows that the stability of the detectors was better than 5%. Therefore the calibration uncertainty was less than 1 MeV around 15 MeV.

Charged particles in coincidence with at least two γ rays were detected by using a forward angle ΔE-E hodoscope. The first stage (ΔE) was an annular silicon strip detector 300 μm thick covering the whole ϕ and a polar angular range θ_{lab}=3°−6°. This detector is divided into eight sectors, each one segmented into nine strips. The second stage (E) consists of eight CsI(Tl) detectors (one for each sector of the silicon detector) 6 cm long with photodiode readout. The silicon detector calibration was obtained using elastic scattering and punching through energies. The CsI(Tl) detectors were calibrated using again elastic scattering and the silicon calibration through energy loss calculations. The known nonlinearity of the CsI(Tl) light response and its dependence from the charge of impinging particles was taken into account by using a neural network approach [21].

A. Charged particle spectra

Fragments stopped in the annular silicon strip detector were charge (Z) identified by using a pulse shape analysis of the signal [22,23]. Contrary to Refs. [22,23], in the present case, ions were impinging on the detector from the junction side. This allows a faster time response of the detectors thus decreasing the problems with the coincidence measurements of γ rays, however a drawback is the larger identification threshold obtained (around 6 MeV/nucleon). In Fig. 1(a) a typical E "rise time" (rise time of the silicon detector signal after the charge preamplifier) scatter plot is reported showing the quality of the charge identification. Particles passing through the silicon stage are identified with the standard ΔE-E technique, see Fig. 1(b).

The velocity spectra of charge identified particles, produced in the reaction with the ^{48}Ca target, detected at θ_{lab}=3° and θ_{lab}=6° are reported in Fig. 2. The velocity was evaluated from the detected energy assuming the mass of the stable isotopes. Similar spectra were obtained also for the ^{46}Ti case. The hole in the middle of the spectra is an artifact

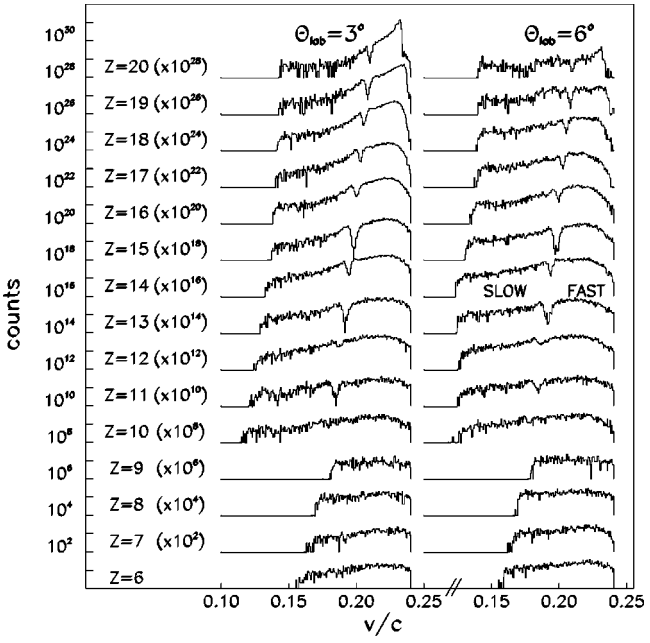

FIG. 2. Velocity spectra for the reaction ^{40}Ca+^{48}Ca measured at $\theta_{lab}=3°$ and $\theta_{lab}=6°$ for different identified charges. The velocity is obtained from the measured energy spectra assuming the mass of the stable ions. The hole in the spectra is produced by the energy threshold of CsI(Tl) detectors and separates the SLOW and FAST selection regions as described in the text.

due to the CsI(Tl) energy threshold. This hole separates two different selection regions named in the following FAST [particles of high energy detected also in the CsI(Tl) scintillators] and SLOW (particles stopped in the silicon detectors). In Fig. 3 the measured angular distribution for each charge, obtained by summing FAST and SLOW contributions, is shown. Looking at Fig. 2 and 3 we can follow the evolution of the reaction mechanisms involved. A quasi-elastic contribution, strongly forward peaked is observed near the projectile charge (note that elastic peak is suppressed by the twofold γ-ray coincidence requirement). More dissipative reactions with a rather constant angular behavior can be observed for charges far from the projectile one. The spectra of Fig. 2 are cut at small velocity by the identification threshold. In particular particles with center of mass (c.m.) velocity ($\beta=0.105$) cannot be seen. Anyhow we can evaluate the presence of such particles in Fig. 4(a) by looking at the rise-time projection of the scatter plot of Fig. 1(a). In this picture we note two bumps, the largest one, labeled as "dissipative reactions," includes the SLOW part of the velocity spectra of Fig. 2, the smaller one, labeled "H.R." (heavy residue), corresponds to the region enclosed in the squared box of Fig. 1(a). The energy projection of this region is peaked around 200 MeV, Fig. 4(b). From simple kinematic considerations, supported also by GEMINI [24] calculations, we expect, around this energy, H.R. produced in incomplete fusion reactions. This assignment is further confirmed by a work on the ^{40}Ca+^{48}Ti reaction [25] at the same beam energy and by constrained molecular dynamics calculations (CoMD) [26] (dots with error bars). The fusionlike products are well separated from dissipative reaction products as can be already seen in Fig. 1(b). The quality of this separation can be evaluated by performing a two Gaussian fit in Fig. 4(a). This fit shows that the contribution of the tail of dissipative events on the H.R. region is rather small (less than 5%) using a cut at −40 in the rise time axis. This cut will be used in the analysis of H.R. later.

B. γ-ray energy spectra

In Fig. 5 are reported the γ-ray multiplicity spectra measured at 90° for the ^{40}Ca+^{48}Ca reaction in coincidence with different type of particles. Such spectra are obtained by normalizing the measured energy spectra to the number of particles detected for the particular cut used. The geometrical solid angle of BaF_2 detectors is taken into account to give the absolute normalization. The effect of the experimental trigger (a multiplicity 2 for γ rays was required, thus strongly suppressing low-multiplicity events) is also included. In the four panels we compare the spectrum measured in coincidence with H.R. and the other selections. The main difference in the spectra is observed in the high-energy region where GDR and bremsstrahlung contributions dominate. As a general trend we note that the SLOW selections show a higher yield than the FAST ones, as expected, due to the higher excitation energy available. The highest yield is observed in coincidence with H.R. For such selection the fit with an exponential function for γ energies larger than 30 MeV (the bremsstrahlung region), gives an inverse slope parameter of 9.2 ± 1.0 MeV, in agreement with previous measurements [29] at similar energies. The energy range of our spectra is not large enough to observe the two slopes evidenced in more recent studies [27,28].

The yield variation observed in Fig. 5 is better quantified in Fig. 6 where the integrals of all the collected spectra for energy higher than 30 MeV are reported (including also the clusters at 45° and 135°). γ rays of these energies are mainly produced via nucleon-nucleon bremsstrahlung and their emission probability can be related to the number of proton-neutron collisions in the first stage of the reaction [3,5]. The probability to generate such γ rays can be connected to the overlap between the two reaction partners or to their impact parameter. Attributing to the Z(15–17)FAST selection an average impact parameter around 7 fm (based on cross-section considerations from the angular distribution of Fig. 3) and using a simple geometrical model [3,5] we obtain, from the measured yield, an average impact parameter of $2-3$ fm for the H.R. This average impact parameter is similar to that obtained with CoMD calculations [26]. The large difference (a factor 4 on average) between the yield observed with H.R. and with SLOW selections, further confirms that different reaction mechanisms contribute to the two regions.

A quite high multiplicity is observed in coincidence with fast particles with charge from 6 to 9. This unexpected high yield can be explained by assuming that this selection includes also projectilelike spectators of incomplete fusion events.

C. Evidences for preequilibrium γ-ray emission and GDR decay

As reported in the Introduction, preequilibrium γ-ray emission has been observed in reactions between nuclei with

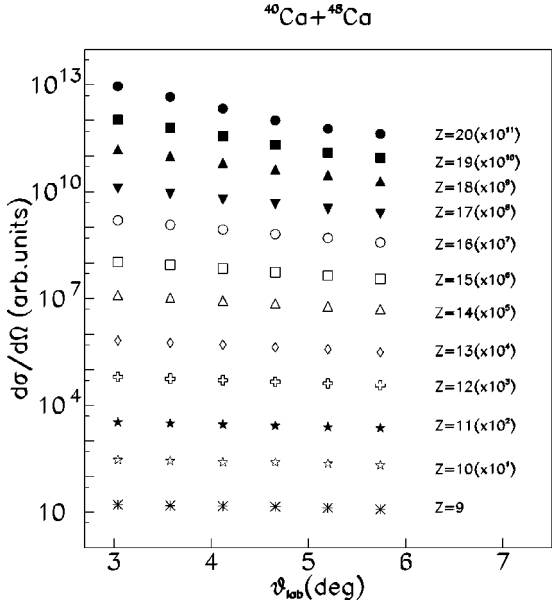

FIG. 3. Angular distributions of charge identified particles for the reaction ^{40}Ca+^{48}Ca.

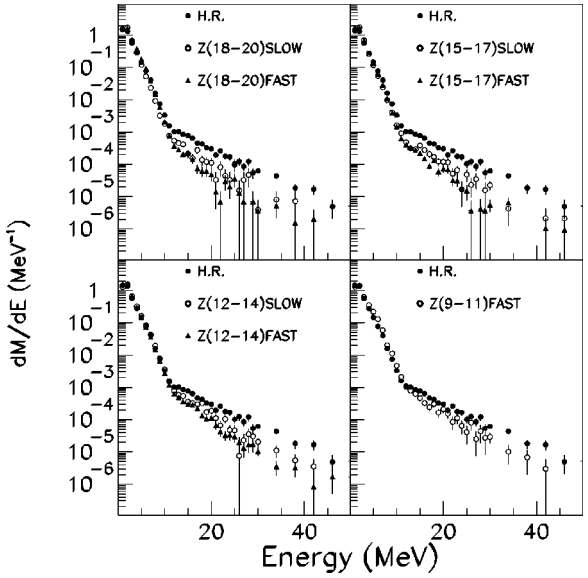

FIG. 5. Comparison between γ-ray multiplicity spectra measured at 90°, for the reaction ^{40}Ca+^{48}Ca, in coincidence with H.R. and the different FAST and SLOW selections of charged particles.

a strong asymmetry in the N/Z ratio [11,12,14–16]. As soon as projectile and target form a dinuclear system, in the very first stages of the collision, nucleons begin to move in order to equilibrate such N/Z ratio. This motion of neutrons against protons is similar to the commonly accepted picture of the GDR excitation and its signature is the emission of γ rays in the region between 8−12 MeV. Such energy is lower than that of the standard GDR because the oscillation axis is approximately given by the sum of the two radii of the interacting nuclei forming the dinuclear system. The ratio between the γ-ray spectra collected for the two reactions can evidence the presence of such preequilibrium effect. Such ratios extracted for spectra collected at different angles and for H.R., SLOW, and FAST selections are plotted in Figs. 7 and 8. In Fig. 8 we can see a clear enhancement in the spectra around 10 MeV at all angles for the H.R. selection. A similar trend but with larger error bars seems to be present also for $Z=18-20$ SLOW selection. A rather flat behavior with very small fluctuations can be seen for $Z=10-14$. The different behavior observed for the various selections and the presence of the enhancement at all angles confirms us that the enhancement is not an artifact produced by gain shift or other experimental problems. A strong enhancement is present also for FAST selections (Fig. 8) particularly pronounced for $Z=15-17$. It is interesting to note the energy shifts of the enhancement with the angle. These shifts could be explained as an evidence of Doppler shift effect even if the energy position of the enhancement, extracted by the spectra ratio, can be strongly influenced by the exponential slope of the spectra. An attempt to extract the apparent Doppler shift failed due to the lack of statistics which did not allow a precise determination of the average position of the enhancement for each angle (we got an error of about 40% on the source velocity).

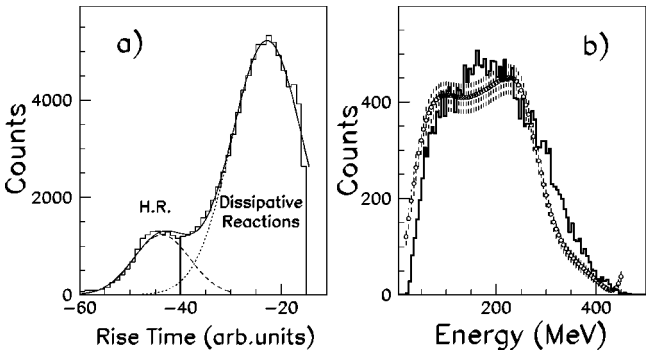

FIG. 4. (a) Projection on the rise time axis of the scatter plot of Fig. 1(a). The line is obtained by performing a two Gaussian fit of the spectrum. The threshold for H.R. selection (line at rise time =−40) is also shown. (b) Experimental energy spectrum of the H.R. selection (full line). The histogram plotted as open point with error bars is a calculation produced using CoMD [26].

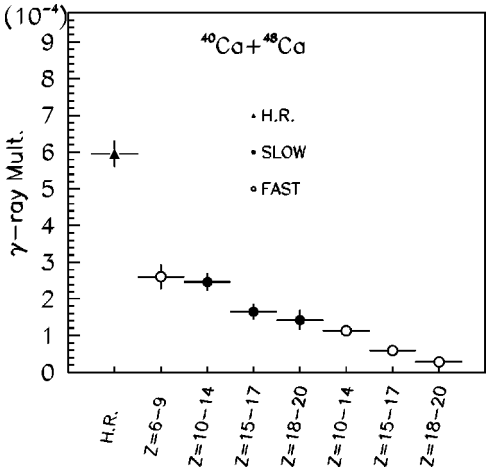

FIG. 6. High energy ($E \geqslant 30$ MeV) γ-ray multiplicity measured for the reaction ^{40}Ca+^{48}Ca in coincidence with different charged particle selections.

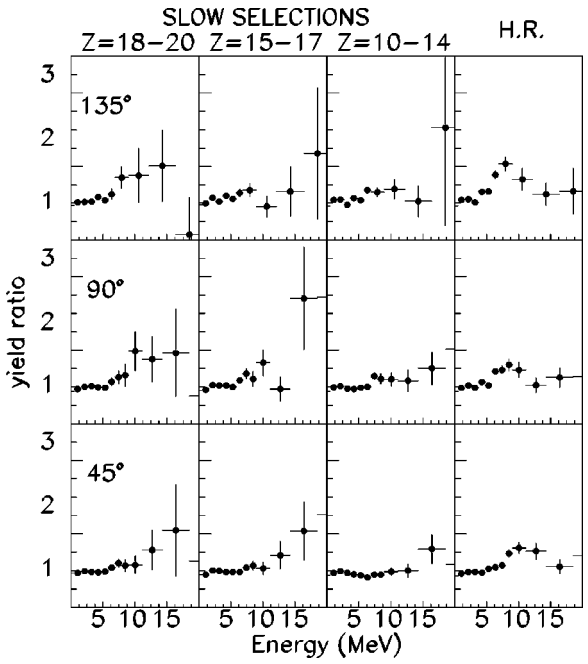

FIG. 7. Ratios between the γ-ray energy spectra measured at different angles in coincidence with SLOW and H.R. selections of charged particles for the reactions ^{40}Ca+^{48}Ca and ^{40}Ca+^{46}Ti.

To perform a good analysis of GDR we must concentrate on the region of the γ-ray energy spectra between 15 and 20 MeV. In this region the low statistics imposes to sum all the γ-ray spectra collected at different angles. This can be done only performing a Doppler shift correction of the spectra. However this correction is not simple for dissipative reactions where at least two γ-ray sources are present, with different velocity. Therefore we can perform the sum of the doppler shifted spectra only for H.R. data mainly produced in fusionlike reactions. For the Doppler shift correction in this case we assume that the γ-ray source moves with the c.m. velocity, as expected for incomplete fusion reactions in nearly symmetric systems [30,31]. In Fig. 9 we show the γ-ray multiplicity spectra in coincidence with H.R. for the two targets obtained in this way. In such a figure, the presence of the GDR γ-ray decay can be observed around 15 MeV. This is better evidenced by comparing the data with a statistical model calculation obtained for the ^{48}Ca target (full line) assuming zero strength for the GDR γ decay (NO GDR). We note a smaller yield in the GDR region for the ^{40}Ca+^{46}Ti reaction (full dots). This yield difference is better evidenced in the inset of Fig. 9 where we plot the ratio between the γ-ray spectra collected in the two measured reactions. We clearly see in this ratio also the persistence of the enhancement around 10 MeV in the reaction ^{40}Ca+^{48}Ca (open dots). The strength of the enhancement is similar to the average strength observed in Fig. 7 for the different detection angles. This means that the velocity of the source generating the enhancement is near the c.m. velocity used to perform the doppler shift correction.

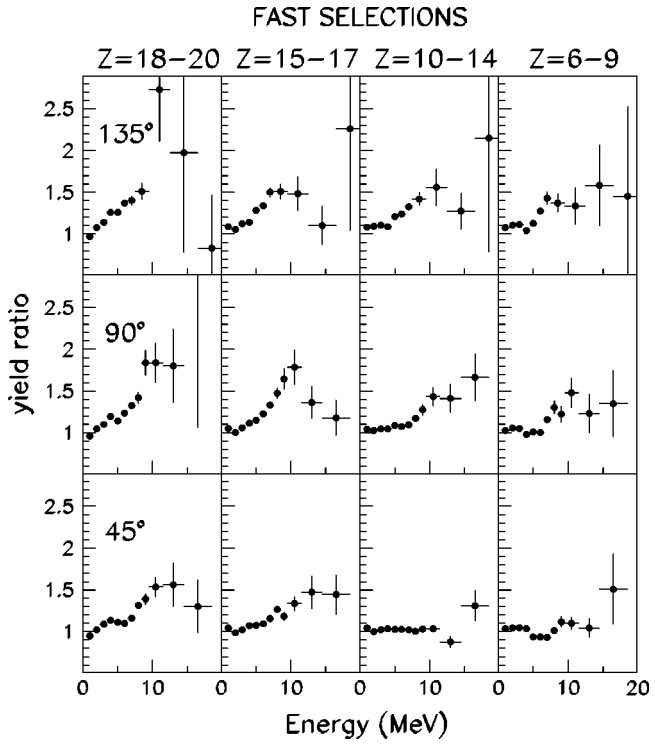

FIG. 8. Ratios between the γ-ray energy spectra as in Fig. 7 measured in coincidence with different FAST selections of charged particles.

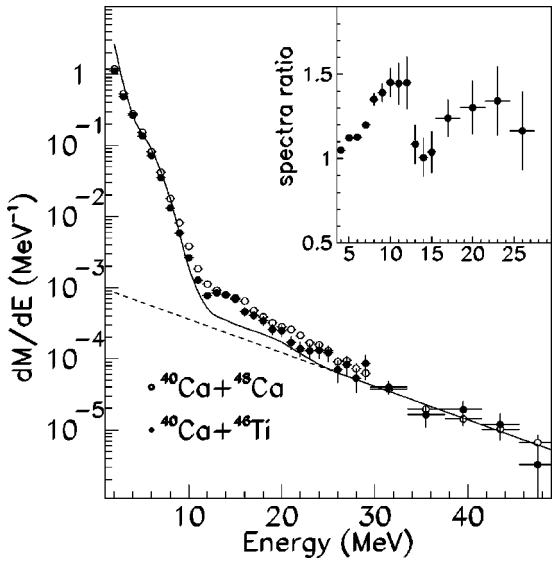

FIG. 9. γ-ray multiplicity spectra for the reactions ^{40}Ca+^{48}Ca (open dots) and ^{40}Ca+^{46}Ti (full dots) measured in coincidence with H.R. Full line is a CASCADE calculation assuming zero strength for the GDR summed to the bremsstrahlung contribution (dashed line). The calculation is folded with the detector response function. In the inset we report the ratio of the two experimental spectra.

III. STATISTICAL MODEL CALCULATIONS

We will concentrate our analysis on the reactions producing the H.R. selected as shown in Fig. 1. In this case, as explained in Sec. II, we can assume that only one major source of γ rays is present, produced in fusion or incomplete-

fusion reactions. As observed in Fig. 5 in these reaction mechanisms we have the population of systems with the highest excitation energy between the investigated ones. This allows the extraction of information on the limiting excitation energy for collective motions in our systems.

A. Source characterization

In order to reproduce the GDR γ-ray emission we have to perform statistical model calculations and the first step for such calculations is the source characterization. We detected only the H.R. produced by the deexcitation of an incomplete fused system. Many particles are emitted from this system before the equilibrium is reached. It is therefore rather difficult to evaluate the excitation energy and mass of the equilibrated compound nucleus. We used experimental data available in literature from Ref. [25] for a similar system ^{40}Ca $+^{48}$Ti at the same beam energy of 25 MeV/nucleon. The average mass of the equilibrated system formed was evaluated in that work by adding the mass of the detected heavy residue to the mass of evaporated particles. The multiplicity distribution of particles, detected in coincidence with heavy residues, was obtained by analyzing their energy spectra and angular distributions in order to separate preequilibrium and statistical contributions. In the same way an average excitation energy of 337 ± 30 MeV after preequilibrium emission was also evaluated. Correcting the ^{48}Ti results mainly for the Q-value differences with respect to our systems, we obtained average excitation energies of 354 MeV and 335 MeV for ^{48}Ca and ^{46}Ti, respectively. We note that the excitation energy evaluation of Ref. [25] was performed assuming that proton and the undetected neutrons carry away the same energy apart from Coulomb effects. This is consistent with our following calculations that give energy spectra with very similar slope for proton and neutrons. A mass of 62 was assumed for both systems. A charge $Z=28$ (29) was assumed for the ^{48}Ca (^{46}Ti) target system. Another approximation was to assume an average spin of $29\hbar$ for both systems computed as 2/3 of their critical angular momentum. The assumed values are in agreement with calculations based on the CoMD model [26]. Assuming a window of impact parameters with average value around 4 fm that well reproduce the energy spectrum of the heavy residue detected [see Fig. 4(b)], such calculation predicts that the largest fragment coming out from the reaction reaches an average mass around 60 after the first $200-300$ fm/c, Fig. 10.

The assumption of a defined excitation energy and mass of the starting system is obviously a strong approximation. One should also include in the calculations some fluctuations of the source characteristics. Anyhow in the following we will show that this error is small and it is not the major source of uncertainties in our analysis.

B. Description of the high-energy statistical code

The most widely used code to compute statistical γ-ray decay is CASCADE [32]. It is a code built to evaluate the compound nucleus decay at relatively low excitation energy. Due to this it considers as a default, apart from γ, only proton (p), neutron (n), and α-particle decays. These assumptions are correct for systems with low excitation energy whereas it is well known that more complex fragments can be evaporated at higher excitation energy [24]. In particular, as shown in Fig. 11(a), we verified using the GEMINI [24] code that for our excited systems the deuteron decay channel is predicted to have a cross section larger than the α-particle one. Even if this very high yield is not experimentally observed in Ref. [25] and in Ref. [33] it has been shown that statistical codes overpredict the yield of such channels, one cannot neglect the contribution of these channels.

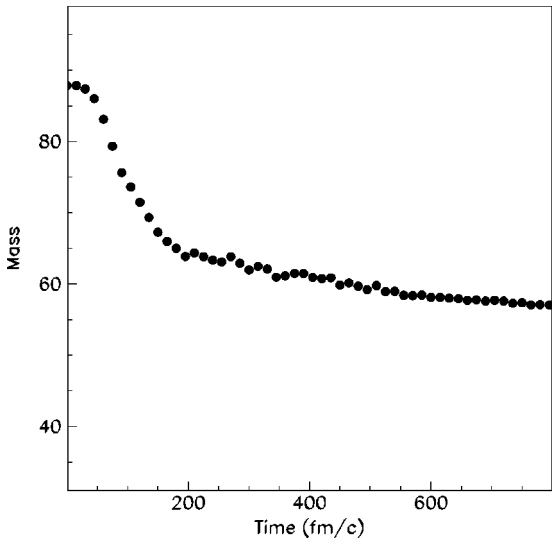

FIG. 10. CoMD simulation showing the mass vs time evolution of the largest fragment produced in the ^{40}Ca+^{48}Ca reaction at 25 MeV/nucleon.

To see the effect of complex fragment emission on the γ-ray spectra we used the fourth particle decay option in CASCADE. This option allows to compute the emission probability of a further particle different from p, n, and α. Allowing for the emission of another fragment we always observe a modification of the GDR γ-ray decay strength. This is similar to the GDR suppression effect observed in Ref. [20] due to energy conservation considerations. As can be seen in

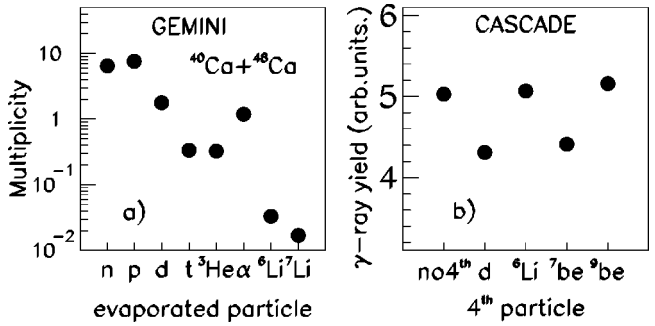

FIG. 11. (a) Light particle multiplicity computed with GEMINI for the decay of a system having mass 62 and excitation energy of 354 MeV populated in the ^{40}Ca+^{48}Ca reaction. (b) γ-ray yield in the GDR region computed using CASCADE and different particles used as fourth decay particle in the program (see text). Calculations were normalized at 4 MeV to be consistent with the experimental data analysis

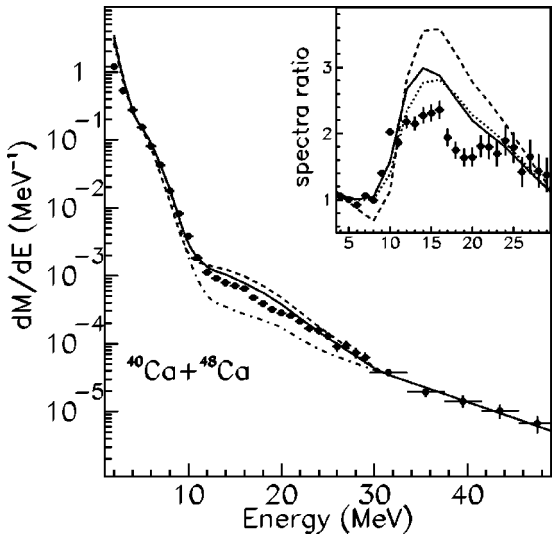

FIG. 12. γ-ray multiplicity spectrum for the ^{40}Ca+^{48}Ca reaction measured in coincidence with H.R. The lines are CASCADE calculations summed to the bremsstrahlung contribution, folded with detector response function and normalized to the data at 4 MeV. Dashed line is a standard calculation with E_{GDR}=16.8 MeV and Γ_{GDR}=15 MeV. Full line is obtained using the same GDR parameters and including also the deuteron decay channel. The dotted line is computed including the deuteron channel and assuming also a mass and isospin dependence of the GDR centroid. The dot-dashed line is the GDR zero strength calculation of Fig. 9 used to linearize experimental data and calculations in the ratio shown in the inset.

Fig. 11(b), the deuteron is the simplest particle that has a large effect on the γ-decay yield. (The total effect of a particular decay channel is due to the average excitation energy subtracted by the particle in the decay chain weighted by its decay probability.) In the case of deuterons we have one of the largest differences because of the high decay probability.

The change in the γ-ray yield can be better evaluated in Fig. 12 where a standard CASCADE calculation (dashed line) is compared with the one obtained using a deuteron as fourth particle (full line). The same GDR parameters were used for both calculations (Γ_{GDR}=15 MeV, E_{GDR}=16.8 MeV, see below). The calculations are normalized to the data around 4 MeV in order to avoid problems due to the preequilibrium effects in the region from 6 to 12 MeV. The difference in the GDR region is better seen in the inset obtained dividing both the experimental data and the calculations by the "NO-GDR" calculation (dot-dashed line) already presented in Fig. 9.

Note that the bump around 20 MeV observed in the linearized plot in the inset of Fig. 9 is produced by the sum of CASCADE and bremsstrahlung terms in the "NOGDR" calculation.

The excited systems considered have an average mass A =62. Following the suggestions of Ref. [35], we used an isospin dependent [34] version of the CASCADE code with the Reisdorf parametrization of the level density. The code was slightly modified by increasing the number of daughter nuclei due to the length of the decay chain (20–30 nucleons can be evaporated).

For such a long decay chain one should also account for the GDR parameter changes along it. There is enough excitation energy to populate the GDR along nearly all the decay steps, and the mass of the effective source ranges from 60 to less than 40 a.m.u. The ground state GDR systematics [2] gives in this mass range a spread of the GDR centroid of about 2 MeV, going from 18.2 MeV for mass 60 to 20.2 MeV for mass 40. This value is obtained by averaging the two contributions $T_<=T$ and $T_>=T+1$, T being the isospin of the level over which the GDR is built.

The energy difference between these components can be high [$\Delta E=60(T+1)/A$ MeV [37]], ΔE=4 MeV has been measured for mass 62 [38]. In reactions with heavy ions, generally, only the $T_<=T$ components is excited in the first step due to isospin conservation. A GDR centroid around 16.8 MeV is reported by experimental studies at high excitation energy both for masses 60 and 40 [35,36]). In our reaction the $T_>$ component of the GDR can be excited in some decay steps, even if with low probability. In order to use a general expression we decided to use the mass dependence of the GDR centroid for $T_<$ levels given by Ref. [2], but normalized to reproduce the 16.8 MeV value for mass 62. We used the Fallieros shift [37] to get the $T_>$ centroid energy. The result of such improved calculations is shown as dotted line in the inset of Fig. 12. With respect to the calculations with fixed E_{GDR}=16.8 MeV (full line) we observe that the effect of this adjustment is a rather small shift of the curve towards higher energies. The large width used in fact washes out the relatively small corrections of the GDR centroid.

In all the above calculations we used a zero value for the isospin mixing parameters. This assumption is justified by the observed restoration of the isospin purity at high excitation energy [39]. Calculations were also folded with the detector response function computed with GEANT3, and in order to account for the bremsstrahlung γ rays, a decreasing exponential function was added to the CASCADE results.

IV. LIMITING GDR EXCITATION ENERGY

In all CASCADE calculations presented up to now a GDR width (Γ_{GDR}) of 15 MeV was used. This is the largest Γ_{GDR} extracted from the fit with a single Lorentzian performed on nuclei around mass 60 populated at high excitation energy [40]. The same width was generally used along the decay chain. We used the constant Γ_{GDR} hypothesis assumed in the standard systematics at high excitation energy. It is evident from Fig. 12 that these calculations largely overestimate the γ-ray yield in the GDR region, therefore a GDR suppression seems present. The simplest way to reproduce such suppression is to assume a GDR sharp cutoff with zero GDR strength above a given excitation energy. We obtained the best fit of the data assuming 260 MeV for E^*_{cutoff}, i.e., 4.7 MeV/nucleon (taking into account that the average mass of the residue at E^*_{cutoff} is reduced to 55 a.m.u.) see Fig. 13 (full line). In order to avoid the influence of the low-energy preequilibrium γ-ray emission evidenced in Sec. II, the χ^2 was evaluated in the energy range from $12 \leqslant E_\gamma \leqslant 25$ MeV. To be consistent with previous studies we used a GDR width Γ_{GDR}=15 MeV constant along the decay chain. On the other hand, due to a strong spin dependence, this saturation width

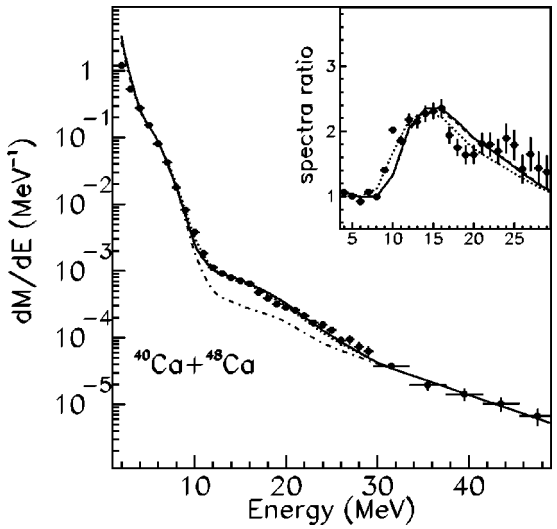

FIG. 13. γ-ray multiplicity spectrum as in Fig. 11. The dot-dashed line is the GDR zero strength calculation used to linearize experimental data and calculations in the ratio shown in the inset. Full line is a best fit of the data obtained assuming a Γ_{GDR} =15 MeV and E^*_{cutoff}=260 MeV. The dashed line is obtained using the smooth cutoff expression discussed in the text. The dotted line is obtained assuming a mass of 70 a.m.u. for the source and E^*_{cutoff}=260 MeV.

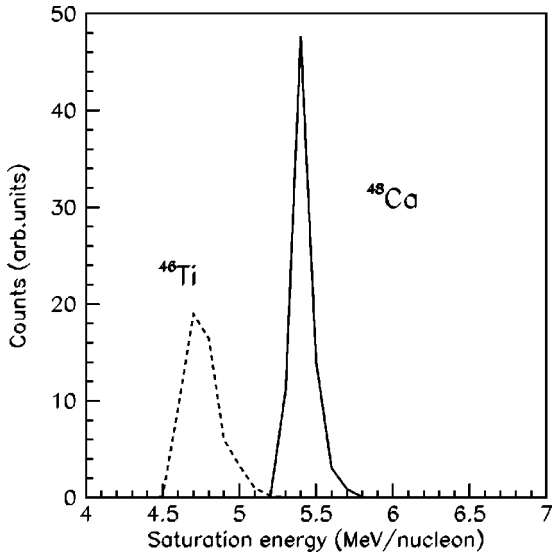

FIG. 14. Saturation excitation energy per nucleon for the reactions ^{40}Ca+^{48}Ca (full line) and ^{40}Ca+^{46}Ti (dashed line) as obtained with the fit performed using the smooth cutoff approximation.

seems to be reached rather soon, around 100 MeV of excitation energy [40], and the use of a GDR width dependence from the excitation energy up to this energy decreases the energy cutoff of only 20 MeV.

A more refined analysis with a smooth cutoff expression is suggested in Ref. [41]. In this reference the GDR suppression is attributed to the impossibility to excite a GDR when the particle decay time of a system is too short with respect to the GDR excitation time. With this assumption the GDR yield is decreased by a factor $\Gamma^{\downarrow}/(\Gamma^{\downarrow}+\Gamma_{ev})$ where $\Gamma^{\downarrow}$ is the spreading width of the GDR and Γ_{ev} is the particle decay width. Using Γ_{ev} as computed by CASCADE, and varying $\Gamma^{\downarrow}$ we obtain the best fit with $\Gamma^{\downarrow}$=6.5 MeV. It is hard to see any difference between the curves obtained with such smooth cutoff (dashed line in Fig. 13), and the one computed with the sharp cutoff approximation (full line in Fig. 13). The cutoff excitation energy can be evaluated in this case as the energy where $\Gamma^{\downarrow}/(\Gamma^{\downarrow}+\Gamma_{ev})=1/2$. We calculated this energy for each decay chain with CASCADE, see Fig. 14, obtaining an average excitation energy around 5.4 MeV/nucleon. Even in this case, we used a Γ_{GDR} constant along the decay chain.

For sake of completeness we discuss also another possible way to explain the GDR strength saturation. One can obtain this result also assuming a Γ_{GDR} increasing with the excitation energy. In this case the strength saturation is due to its spread over a large energy range. After long discussions [42–44] this hypothesis was rejected in Ref. [5] by the comparison with experimental data. However we tested also this possibility as suggested again in Ref. [45]. In Ref. [46] the increase of the GDR width is connected to the increase of the particle decay width by the expression $\Gamma_{GDR}=\Gamma^{\downarrow}+2*\Gamma_{ev}$. Applying this recipe we obtained a poor agreement, dashed line in Fig. 15, the γ yield being largely overestimated. Another expression is suggested in Ref. [44] $\Gamma_{GDR}=4.8+0.0026(E^*)^{1.6}$ MeV. This expression follows the GDR width behavior in the mass region of Sn isotopes. To better reproduce the systematic at low excitation energy for mass 60, we modified this expression including a linear spin dependence ($\Gamma_{spin}=0.06*E^*$ MeV) saturated at 100 MeV (at this energy the critical angular momentum of the system is already reached). With this approximation, we obtain a yield reduction with respect to the previous calculation, however, we are still overestimating the experimental results, full line in Fig. 15.

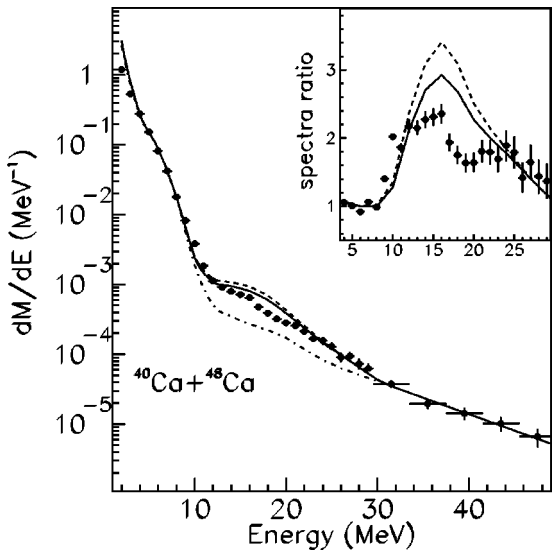

FIG. 15. γ-ray multiplicity spectrum as in Fig. 11. The dot-dashed line is the GDR zero strength calculation used to linearize experimental data and calculations in the ratio shown in the inset. The dashed line is obtained by increasing the GDR width with excitation energy as in Ref. [46]. Full line is obtained following Ref. [44] with modifications as explained in the text.

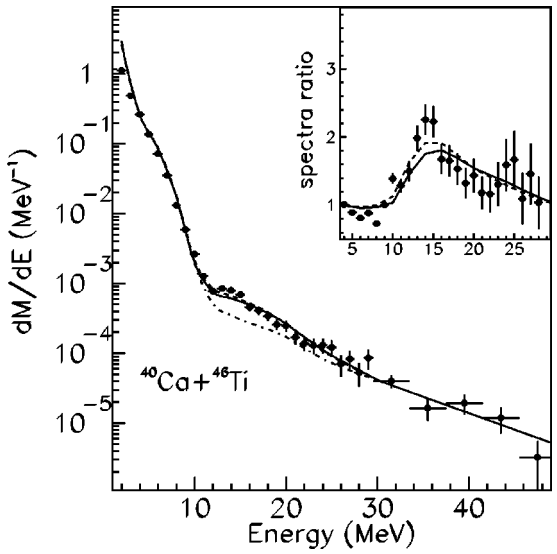

FIG. 16. Same as Fig. 14, but for the ^{40}Ca+^{46}Ti reaction. The dashed line is the fit obtained at constant Γ_{GDR}=15 MeV giving a sharp cutoff E^*_{cutoff}=200 MeV. The full line is computed assuming a smooth cutoff as shown in Fig. 14.

The ^{46}Ti data appear to be in agreement with the ^{48}Ca observations even if a smaller E^*_{cutoff} is obtained. In the hypothesis of sharp cutoff we find the best χ^2 at E^*_{cutoff} =200 MeV. This result is obtained assuming a GDR strength S=0.8 energy weighted sum rule (EWSR) (dashed line in Fig. 16), larger strength values give unreasonably low cutoff energies. Considering the average mass of the system at 200 MeV excitation energy (53 a.m.u.) we obtain E^*_{cutoff} =3.8 MeV/nucleon. Using the smooth cutoff approximation the best fit is obtained with $\Gamma^{\downarrow}$=5.2 MeV, S=0.8 EWSR, full line in Fig. 16. In this case we have to use again S=0.8 EWSR in order to obtain reasonable values for the $\Gamma^{\downarrow}$ (in fact a value larger than the ground state GDR width is expected). The corresponding saturation excitation energy for the GDR is plotted as dashed histogram in Fig. 14. We obtain approximately 4.7 MeV/nucleon.

The extracted limiting excitation energy does not depend strongly on the mass and excitation energy adopted for the initial sources. This is shown in Fig. 13 where we can also compare the calculations using E^*_{cutoff}=260 MeV (full line) with another calculation performed assuming mass 70 instead of 62 a.m.u. (dotted line). This last calculation is slightly shifted towards lower energies. In this case a larger cutoff energy (around 280 MeV instead of 260) is necessary to better reproduce the data. However, because of the higher mass, the variation in terms of excitation energy per nucleon is negligible. Similar small variations were also observed by 10% changes of the initial excitation energy. A larger error comes from the bremsstrahlung estimation. On ^{48}Ca data a change of the bremsstrahlung yield inside the error bars produces a variation of about 10% on the average limiting excitation energy per nucleon. Due to the low statistics, the bremsstrahlung evaluation for the ^{46}Ti target was not possible. We used the same exponential function as for the ^{48}Ca data. This gives the systematic error estimated to be below 5% due to the different number of n-p collisions.

A further improvement of the calculations could be obtained if all available decay channels would be added to CASCADE. This task will be the object of a future study. However the insertion of other channels should give only second order corrections. In fact other channels will decrease the decay probability of γ but also of deuterons. Due to the generally lower decay probability of other decay channels [see Fig. 11(a)] we can say that part of their effect is already included in the deuteron decay channel. Any additional decay channel, in any case, would increase the energy cutoff extracted and the maximum excitation energy per nucleon.

The same effect is expected for small contaminations of dissipative reactions. In fact such contaminations with γ rays produced by lower excitation energy systems decreases the detected GDR γ-ray multiplicity (see Fig. 6). The fit of such lower multiplicity spectra will give a cutoff excitation energy lower than the real one.

We have also to observe that the smooth cutoff expression used from Ref. [41] is in principle exact only for the first decay step of a nucleus in which the GDR is not already excited. Corrections to this expression should be used as suggested in Ref. [47] for the whole decay chain. In the case of ^{48}Ca only about two decay steps are on average necessary to reach the E^*_{cutoff}, however, the reduction factor of the smooth cutoff could influence other decay steps. In Ref. [47] after few decay steps the correction is dropped out because the time of GDR excitation is compared with the lifetime of the system obtained by summing the time of all decay steps. Using such correction one should find a smaller value of the saturation excitation energy but in any case higher than the one obtained with the sharp cutoff expression.

The errors on the performed analysis are in summary comparable to the dispersion of the results obtained with the different hypothesis performed (sharp or smooth cutoff). Using the values obtained with the smooth cutoff approximation, we conclude that we observe a GDR saturation around 5.4±0.5 MeV and 4.7±0.9 MeV, respectively, for ^{48}Ca and ^{46}Ti targets.

V. CONCLUSIONS

In this work we have shown the amount of information on reaction mechanisms and on the status of the excited nuclear matter that can be extracted by the γ-ray spectra measured in coincidence with charged particles in reactions at high beam energy (at 25 MeV/nucleon). In more detail, the high-energy γ rays, mainly produced via nucleon-nucleon bremsstrahlung, have been used to verify the average impact parameter of the reaction channel analyzed. From the comparison of γ-ray spectra produced in reactions with different values of the N/Z ratio between projectile and target, we obtained the evidence of the excitation of the so called "molecular dynamical dipole" observed for the first time in different final reaction channels of a given collision. We also tested the collective behavior of the excited nuclear matter by analyzing the GDR γ-ray decay.

Regarding this last point, an accurate work was necessary in order to evaluate the statistical contribution at high excitation energy and many effects were included. The limiting

excitation energy observed here, around 5 MeV/nucleon, is higher than previous measurements for mass 110 (2.5 −3 MeV/nucleon) [5,6]. The excitation energy extracted is close to the energy where signals of the liquid-gas phase transition were claimed to be present [7], for systems around mass 200. However, as emphasized in the Introduction, these signals are sensitive to the mass of the system. Therefore the observed difference is most probably the signature of this size effect already observed in the caloric curve analysis [9]. A comparison with multifragmentation studies of small size systems is necessary to better understand this point.

Another interesting aspect is the different GDR strength extracted by fitting the γ-ray spectra for the two reactions analyzed. This difference is about 20% and could be connected to the observed preequilibrium emission. Even if this emission is more evident in the γ-ray spectra around 9 MeV, some contribution could be present also in the statistical GDR region affecting the strength measurement. To this respect although the ^{46}Ti data are characterized by a larger statistical error, they probably give a better estimation of the limiting GDR excitation energy. However, there is possible also an isospin dependence of the limiting temperature justified by the isospin term of the nuclear matter equation of state.

[1] A. Di Pietro *et al.*, Z. Phys. A **350**, 199 (1994).
[2] J. J. Gaardhøje, Annu. Rev. Nucl. Part. Sci. **42**, 483 (1992); A. van der Woude, Prog. Part. Nucl. Phys. **18**, 217 (1987); K. A. Snover, Annu. Rev. Nucl. Part. Sci. **36**, 586 (1986).
[3] H. Nifenecker and J. A. Pinston, Annu. Rev. Nucl. Part. Sci. **40**, 113 (1990).
[4] A. Bonasera, M. Bruno, C. O. Dorso, and P. F. Mastinu, Riv. Nuovo Cimento **23**(2), 1 (2000).
[5] T. Suomijarvi *et al.*, Phys. Rev. C **53**, 2258 (1996).
[6] J. J. Gaardhøje, A. M. Bruce, and B. Herskind, Nucl. Phys. **A482**, 121c (1988).
[7] M. D' Agostino *et al.*, Phys. Lett. B **473**, 219 (2000).
[8] S. Tudisco *et al.*, Europhys. Lett. **58**, 811 (2002).
[9] J. B. Natowitz *et al.*, Phys. Rev. C **65**, 034618 (2002).
[10] G. Cardella *et al.*, in *Proceedings of the Conference Bologna 2000: Structure of the Nucleus at the Dawn of the Century, Bologna*, edited by G. C. Bonsignori,M. Bruno, A. Ventura, and D. Vretenar (World Scientific, Singapore, 2000), p. 305.
[11] S. Flibotte, P. Chomaz, M. Colonna, M. Cromaz, J. DeGraaf, T. E. Drake, A. Galindo-Uribarri, V. P. Janzen, J. Jonkman, S. W. Marshall, S. M. Mullins, J. M. Nieminen, D. C. Radford, J. L. Rodriguez, J. C. Waddington, D. Ward, and J. N. Wilson, Phys. Rev. Lett. **77**, 1448 (1996).
[12] M. Cinausero *et al.*, Nuovo Cimento **111**, 613 (1998).
[13] L. Campajola *et al.*, Z. Phys. A **352**, 421 (1995).
[14] M. Sandoli *et al.*, Eur. Phys. J. A **6**, 275 (1999).
[15] F. Amorini, M. Cabibbo, G. Cardella, A. Di Pietro, P. Figuera, A. Musumarra, M. Papa, G. Pappalardo, F. Rizzo, and S. Tudisco, Phys. Rev. C **58**, 987 (1998).
[16] M. Papa, F. Amorini, M. Cabibbo, G. Cardella, A. Di Pietro, P. Figuera, A. Musumarra, G. Pappalardo, F. Rizzo, and S. Tudisco, Eur. Phys. J. A **4**, 69 (1999).
[17] M. Papa, F. Amorini, A. Di Pietro, G. Cardella, P. Figuera, A. Musumarra, G. Pappalardo, F. Rizzo, and S. Tudisco (unpublished).
[18] G. Cardella *et al.*, in *Proceedings of the IX International Conference on Nuclear Reaction Mechanisms, Varenna, 2000*, edited by E. Gadioli (Dipartimento di Fisica, Università di Milano, 2000), p. 427.
[19] A. Musumarra, G. Cardella, A. Di Pietro, S. L. Li, M. Papa, G. Pappalardo, F. Rizzo, S. Tudisco, and J. P.S. Van Schagen, Nucl. Instrum. Methods Phys. Res. A **370**, 558 (1996).
[20] A. Di Pietro *et al.*, Nucl. Phys. **A689**, 668 (2001).
[21] M. Iacono Manno and S. Tudisco, Nucl. Instrum. Methods Phys. Res. A **443**, 503 (2000).
[22] G. Paush *et al.*, Nucl. Instrum. Methods Phys. Res. A **365**, 176 (1995), and references therein.
[23] J. Lu, P. Figuera, G. Cardella, A. Di Pietro, A. Musumarra, M. Papa, G. Pappalardo, F. Rizzo, and S. Tudisco, Nucl. Instrum. Methods Phys. Res. A **472**, 374 (2001).
[24] R. J. Charity *et al.*, Nucl. Phys. **A483**, 371 (1988).
[25] T. M. V. Bootsma, G. J. van Nieuwenhuizen, P. F. Box, R. Kamermans, P. G. Kuijer, C. T. A. M. de Laat, C. J. W. Twenhofel, P. Decowski, and K. A. Griffioen, Z. Phys. A **359**, 391 (1997).
[26] M. Papa, T. Maruyama, and A. Bonasera, Phys. Rev. C **64**, 024612 (2001); M. Papa *et al.*, *ibid.* **68**, 034606 (2003).
[27] D. G. d'Enterria *et al.*, Nucl. Phys. **A681**, 291 (2001).
[28] R. Alba *et al.*, Nucl. Phys. **A681** 339 (2001).
[29] P. Sapienza *et al.*, Nuovo Cimento Soc. Ital. Fis., A **111A**, 999 (1998).
[30] H. Morgenstern, W. Bohne, W. Galster, K. Grabisch, and A. Kyanowski, Phys. Rev. Lett. **52**, 1104 (1984).
[31] S. K. Samaddar, J. N. De, and D. Sperber, Phys. Rev. C **46**, 2631 (1992).
[32] F. Pühlhofer, Nucl. Phys. **A280**, 267 (1977); M. N. Harakeh (private communication).
[33] R. J. Charity, L. G. Sobotka, J. F. Dempsey, M. Devlin, S. Komarov, D. G. Sarantites, A. L. Caraley, R. T. deSouza, W. Loveland, D. Peterson, B. B. Back, C. N. Davids, and D. Seweryniak, Phys. Rev. C **67**, 044611 (2003).
[34] M. N. Harakeh *et al.*, Phys. Lett. B **176**, 279 (1986).
[35] M. Kicinska-Habior, K. A. Snover, C. A. Gossett, J. A. Behr, G. Feldman, H. K. Glatzel, J. A. Gundlach, and E. F. Garman, Phys. Rev. C **36**, 612 (1987).
[36] G. Feldman, K. A. Snover, J. A. Behr, C. A. Gossett, J. H. Gundlach, and M. Kicinska-Habior, Phys. Rev. C **47**, 1436 (1993).
[37] R. Ö. Akyüz and S. Fallieros, Phys. Rev. Lett. **27**, 1016 (1971).
[38] T. J. Bowles, R. J. Holt, H. E. Jackson, R. D. McKeown, A. M. Nathan, and J. R. Specht, Phys. Rev. Lett. **48**, 986 (1982).
[39] J. A. Behr *et al.*, Phys. Rev. Lett. **70**, 3201 (1993).
[40] B. Fornal *et al.*, Z. Phys. A **340**, 59 (1991).
[41] P. F. Bortignon, A. Bracco, D. Brink, and R. A. Broglia, Phys. Rev. Lett. **67**, 3360 (1991).

[42] J. Kasagi *et al.*, Nucl. Phys. **A538**, 585c (1992).
[43] See, for instance, W. E. Ormand, P. F. Bortignon, R. A. Broglia, and A. Bracco, Nucl. Phys. **A614**, 217 (1997); A. Bonasera *et al.*, *ibid.* **A569**, 215c (1994); Ph. Chomaz, *ibid.* **A569**, 203c (1994).
[44] A. Smerzi, M. Di Toro, and D. M. Brink, Phys. Lett. B **320**, 216 (1994).
[45] M. P. Kelly, K. A. Snover, J. P. S. vanSchagen, M. Kicinska-Habior, and Z. Trznadel, Phys. Rev. Lett. **82**, 3404 (1999).
[46] Ph. Chomaz, Phys. Lett. B **347**, 1 (1995).
[47] K. A. Snover, Nucl. Phys. **A687**, 337c (2001).